Geotechnical Aspects of Underground Construction in Soft Ground – Ng, Huang & Liu (eds)
 ISBN 978-0-415-48475-6

Three-dimensional finite element analysis of diaphragm walls for top-down construction

J. Hsi, H. Zhang & T. Kokubun
SMEC Australia Pty Ltd, Sydney, NSW, Australia

ABSTRACT: The Tugun Bypass Tunnel in Gold Coast, Australia was constructed using diaphragm walls with the top-down cut-and-cover method to allow simultaneous construction of an airport runway extension above the tunnel, whilst excavation of the tunnel continued underneath. The tunnel was built in an environment of high groundwater table and deep deposits of alluvial and estuarine soils with the toes of the walls founded in soil deposits. There was a potential risk for differential settlements between the diaphragm wall panels, caused by the runway fill placed over the tunnel roof during excavation. Three-dimensional numerical modelling was undertaken to predict the differential settlements of the tunnel with considerations of varying subsurface profile, staged excavation and dewatering, non-uniform loading and complex soil-structure interaction. Field instrumentation and monitoring was implemented to confirm numerical predictions.

1 INTRODUCTION

The 7 km long Tugun Bypass forms part of the Pacific Highway, and connects south-east Queensland to northern New South Wales, Australia. One of the key features of the project was a tunnel of about 334 m in length (Ch5588 to Ch5922.4), constructed below the proposed runway extension of the Gold Coast Airport. Figure 1 presents the project route plan showing the locality of the project.

Figure 1. Project route plan.

As the tunnel was to be constructed in the proximity of the airport runway, there was a strict height restriction for the construction activities. Low headroom plant and equipment were chosen to construct the diaphragm walls for the cut and cover tunnel. As the construction of the runway extension coincided with the tunnel construction, the top-down construction method was adopted.

The subsurface of the tunnel site comprised mainly alluvial and estuarine soils up to depths of about 35 m underlain by weathered rock of Neranleigh Fernvale formation. To minimize construction costs, the diaphragm walls were founded in soil deposits which were subjected to settlement under the loading from the runway extension.

Excessive differential settlement of the diaphragm walls could overstress the tunnel structure and affect the tunnel serviceability. Detailed numerical modelling was carried out using the finite element package PLAXIS 3D Foundation (Version 1.6) where the spatial subsurface variation and non-uniform loading patterns could be taken into consideration.

Instrumentation and monitoring were undertaken to demonstrate the field performance, which was then compared with the numerical predictions.

2 SITE GEOLOGY

The tunnel was situated in a flood plain which was subjected to periodical flooding. The geology of the site comprised Neranleigh Fernvale Beds overlain by Cenozoic estuarine and coastal deposits. These

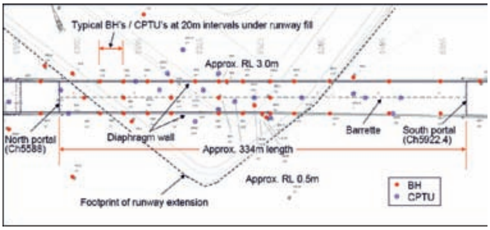

Figure 2. Site investigation plan.

deposits were up to 35 m in thickness, comprising river gravels, sands and clays, and flood plain and tidal delta muds and silts. At the tunnel location, the subsurface horizons consisted of dune sands, "Coffee Rock" (local term given to cemented silty sands), estuarine interbedded clays and sands, and residual soils derived from the weathered bedrock. Groundwater was slightly saline due to the close proximity to the ocean. The water table was influenced by both tidal movements and rainfall events recharging Cobaki Broadwater. Due to low-lying ground surfaces, potentials existed for acid sulphate soils.

3 GEOTECHNICAL MODEL

As the subsurface conditions varied spatially along the length and width of the tunnel, extensive site investigations using boreholes (BH) and piezocones (CPTU) were undertaken at the wall and barrette locations. Within the footprint of the runway extension, the investigations were done at a spacing of approximately 20 m intervals. The plan of the site investigation is shown in Figure 2.

The geotechnical model of the site included subsurface stratigraphy and geotechnical parameters. The subsurface was divided into discrete soil units, classified according to material type and consistency or density and is summarized as follows (top down):

- Top soil – thin skinned (<1 m) comprising peaty sandy organic topsoil, having loose consistency. The ground surface was marshy and generally untrafficable;
- Dune sands – a sequence of generally loose to very loose sands of up to about 8 to 10 m in thickness, fine to medium grained sands;
- "Coffee Rock" (CR) – a sequence of medium dense to very dense cemented silty sands of about 7 to 10 m in thickness with occasional loose consistency;
- Estuarine – a sequence of about 15 m thickness comprising shell fragments, sand and silty sand, clay and sandy clay, silt and clayey silt, clayey silty sand and gravels. Relative density varied from very loose to dense, and consistency varied from firm to very stiff;
- Residual soil – comprising clay and silty clay with some sands, and with residual fragments of extremely weathered and extremely low strength interbedded argillite and greywacke of the Neranleigh Fernvale Beds. The thickness ranged between about 1 m and 6 m;
- Bedrock – comprising extremely weathered to moderately weathered and extremely low to low strength interbedded argillite and greywacke, having an irregular contact with the overlain residual material at a depth of approximately 30 to 35 m.

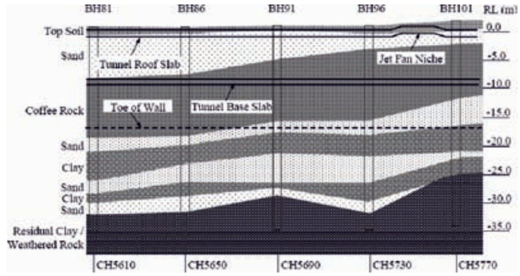

Figure 3. Subsurface profile.

Table 1. Typical soil profile and key geotechnical parameters.

RL (m)	Soil	ϕ' (deg)	k (m/day)	E_{50}^{ref} & E_{oed}^{ref} (MPa)	E_{ur}^{ref} (MPa)
0.5	Sand (VL)	30	1.0	10	30
−4.0	CR (MD)	32	0.1	50	150
−11.2	CR (D)	34	0.1	80	240
−13.5	Sand (L)	32	1.0	30	90
−17.5	Clay (St)	28	1×10^{4}	10	30
−21.1	Sand (L)	32	1.0	30	90
−23.0	Clay (F)	24	1×10^{-4}	7	21
−28.6	Clay (VSt)	29	1×10^{-4}	25	75
−30.8	Bedrock	–	–	–	–

Note: RL (reduced level) is at top of each layer; VL is very loose; L is lose; MD is medium dense; D is dense; F is firm; St is stiff; VSt is very stiff; ϕ' is drained friction angle; k is permeability; E_{50}^{ref} is secant Young's modulus at a reference pressure of 100 kPa; E_{oed}^{ref} is tangent Young's modulus for primary odometer loading at a reference pressure of 100 kPa; and E_{ur}^{ref} is unloading/reloading Young's modulus at a reference pressure of 100 kPa. Refer to PLAXIS manual for Hardening Soil (HS) model.

The subsurface profile based on the boreholes along the centre line of the tunnel is presented in Figure 3. The geotechnical parameters for each of the units were determined from interpretation of the field and laboratory test results, and based on local experience. The typical soil profile and key geotechnical parameters assumed are shown in Table 1. The ground surface level was approximately at RL 0.5 m and the groundwater table was at the surface.

4 ISSUES AND CONSTRAINTS

Construction of a tunnel in soft ground at shallow depths is conventionally undertaken using the "cut and cover" method. However, to allow for construction of the runway extension that occurred concurrently with the tunnel excavation, the top-down construction method had to be adopted. Diaphragm walls and cast in situ tunnel roof slabs had been chosen to facilitate the construction requirements and time constraints. Figure 2 shows the footprint of the runway extension oblique to the tunnel alignment.

Following the handover of ground surface, up to 2–3 m of fill for the airport runway extension was placed above the tunnel roof. Loads acting over the entire width of the roof slabs were transferred directly to the diaphragm walls and the barrettes. The site investigations revealed presence of estuarine deposits consisting of loose materials below the toe of the walls. Therefore, there was a potential for the tunnel to settle during excavation. One of the critical issues was the differential settlements between the walls and the central barrettes, and along the walls. These differential settlements could potentially induce significant stresses in the roof structures and in the walls.

Other issues in relation to the tunnel construction are listed below:

- "Obstacle Limitation Surface (OLS)" – applied at both ends of the runway to provide safe airspace for approaching aircrafts. This required all construction activities to be undertaken within a headroom of as low as 8 m. Use of cranes or heavy-lifting equipment was only allowed outside the airport operating hours;
- High groundwater level – due to its close proximity to the sea and Cobaki Broadwater. The groundwater was practically at the ground surface level. Reliable dewatering system was essential during excavation;
- Environmental requirements – strict environmental controls were enforced such that drawdown of the groundwater table outside the diaphragm walls was insignificant. Also, all acidic sulphate soils excavated from the tunnel had to be dried and neutralized with lime prior to placement as fill in embankments.

5 CONSTRUCTION METHOD

Suitable construction methods were chosen to address the issues and constraints mentioned above. In order to adhere to the OLS requirements, special low headroom hydraulic grab (Leibherr HS852HD) and 2.8 m wide trench cutter (CBC25) were used. The guide walls were

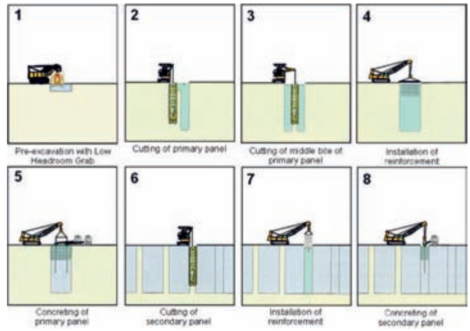

Figure 4. Diaphragm wall construction sequence (courtesy of Bauer/Piling Contractors).

built first followed by construction of the 6 m wide primary panels (Steps 1 to 5 of Figure 4) and 2.8 m wide secondary panels (Steps 6 to 8). The open trench was supported by mixture of bentonite slurry, when the cutter undertook full excavation (Steps 2 to 3 and 6). A steel reinforcement cage was lowered when the panel was excavated to full depth (Steps 4 and 7). Concreting of the panels was then achieved by the tremie method (Steps 5 and 8). Figure 4 presents the construction sequence of the diaphragm wall.

Following completion of the diaphragm walls and barrettes, dewatering and excavation commenced inside the walls. Excavation was initially undertaken to depths of up to about RL −2 m to allow for construction of the roof slab. Water-tight membrane was installed as part of the water-proofing system. When the roof slab was completed, it was backfilled and the site was cleared for handover to the Gold Coast Airport. These activities commenced in April 2006 after environmental approvals were granted, and were completed by November 2006 which was the scheduled date of handover of the site surface. Excavation below the runway extension continued through to January 2007, and the remaining construction of the tunnel continued.

6 STRUCTURAL DETAILS

The tunnel structure consisted of diaphragm walls and barrettes located at the centre of the tunnel. The diaphragm walls were 1 m in thickness, and extended from the Northern Portal (Ch5588) to the Southern Portal (Ch5922.4). The walls were installed to the depth of RL −17 m, from the top of the guide wall at RL 2 m. The internal width between the diaphragm walls ranged from about 25.7 m at the northern portal to 28 m at the southern portal. Barrettes were 0.8 m thick and 2.8 m wide with a clear spacing of 2.8 m throughout the central axis of the tunnel, extending to RL −17 m in depth. These structures had a 100 year design life, using N-grade reinforcing

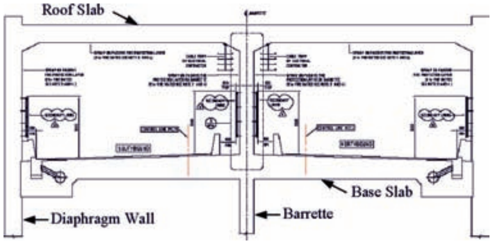

Figure 5. Typical tunnel cross section.

steels and 50 MPa high strength concrete. There were no mechanical 'joints' at the interface of the primary and secondary panels in the longitudinal direction. However, the barrettes and the diaphragm walls were rigidly connected to the 1 m thick roof slab. There were three jet fan niches where the roof slab was slightly elevated. The base slab was also 1 m thick with a founding level ranging from RL −5.5 m to RL −9.5 m. Figure 5 shows the typical cross section of the tunnel.

7 DESIGN CONSIDERATIONS

Geotechnical design of the tunnel was required to satisfy the following three key issues:

- Excavation support during construction – the diaphragm wall structures were designed to ensure stability of the excavation. Issues included structural design of the walls, base heave, hydraulic uplift, piping, and liquefaction;
- Long term stability of the tunnel – buoyancy of the tunnel when the groundwater table was close to the surface;
- Serviceability assessment due to settlement of the tunnel during construction – the tunnel was subjected to loading from airport runway fill which resulted in settlements. The influences of differential settlements on structural capacity were assessed.

8 NUMERICAL MODELLING

8.1 *Two-dimensional numerical modelling*

Design of the tunnel was initially undertaken using the finite element software PLAXIS (Version 8.4) at selected sections. This numerical package was used to analyze two-dimensional plane-strain problems involving complex soil-structure interaction for the design of the structural members. Structural beam elements were used to simulate the diaphragm walls. Global factor of safety during each of the construction stages was calculated based on the c'-φ' reduction method to ensure the minimum FoS was achieved. The software allowed modelling of construction sequence, changing groundwater levels, and varying subsurface conditions across the width of the tunnel.

8.2 *Three-dimensional numerical modelling*

A three-dimensional numerical modelling package, PLAXIS 3D Foundation (Version 1.6), was employed to predict the settlements of the tunnel caused by runway fill loading and excavation. Due to the limitation of the program, settlement analyses were undertaken in sections, each of approximately 40 to 60 m in length. The major advantages of the 3D modelling were as follows:

- Ability to model the physical dimensions of the wall and barrette structures. This improved the accuracy of settlement prediction, as it accounted for longitudinal stiffness of the tunnel which assisted in load redistribution and toe resistance of the structures;
- Ability to simulate 3D load distribution where the runway fill was placed oblique to the longitudinal axis of the tunnel;
- Ability to model 3D subsurface profile based on probe holes at discrete locations;
- Ability to simulate dewatering within the tunnel excavation area.

The Hardening Soil (HS) model was considered most appropriate to simulate soil behaviour in an open excavation. The HS model took into account unloading and reloading behavior and irreversible plastic strains of soil. The HS stiffness parameters were defined with respect to a reference pressure of 100 kPa. The key parameters included E_{50}^{ref}, E_{oed}^{ref}, and E_{ur}^{ref} as shown in Table 1. The published data indicate the ratio of E_{oed}^{ref} to E_{50}^{ref} is about 0.7 to 1.4 and the ratio of E_{ur}^{ref} to E_{50}^{ref} varies from 2 to 4. The analysis adopted $E_{50}^{ref} = E_{oed}^{ref}$, and $E_{ur}^{ref} = 3E_{50}^{ref}$.

Presented here is a 41.2 m long section of the tunnel between Ch5728.8 and Ch5770. This section of the tunnel was of the "deepest" location of the tunnel, beneath the thickest layer of the runway fill, and underlain by sloping bedrock level and changing clay thickness. A jet fan niche of approximately 12 m long also lied within the centre of this section which had also been incorporated in the model. Within this chainage range, there were seven boreholes. Due to the capacity of the program, four representative boreholes, which were evenly distributed spatially, were selected for the analysis. The assumed subsurface profiles are shown in Table 2.

8.3 *Assumptions of analysis*

The construction sequence was considered in the analysis to simulate the load transfer from the runway fill to the diaphragm walls. The assumed construction sequence is described below:

1. Application of loads exerted on the virgin ground from the working platform built to RL 2 m (for construction of the guide walls) and construction load of 10 kPa;

Table 2. Subsurface profiles.

Borehole Location Chainage	#1 LHS 5730	#2 RHS 5737	#3 LHS 5757	#4 Centre 5768	Soil type (density/ consistency)
Unit	RL at top of each layer				
1	0.5	0.5	0.5	0.5	Sand (VL)
2	−4.8	−3.4	−5.0	−2.8	CR (MD)
3	−10.8	−14.4	−9.8	−9.7	CR (D)
4	−13.8	−15.9	−12.6	−11.7	Sand (L)
5	−17.8	−17.1	−17.5	−17.5	Clay (St)
6	−24.3	−21.8	−20.8	−17.5	Sand (L)
7	−27.3	−25.1	−21.8	−18.0	Clay (F)
8	−33.3	−30.8	−25.0	−25.2	Clay (VSt)
9	−36.3	−32.0	−27.4	−27.4	Bedrock

Note: LHS is left hand side of tunnel facing increasing chainage direction; RHS is right hand side of tunnel; and Centre is centre line of tunnel.

2. Installation of diaphragm walls and barrettes to RL −17 m;
3. Removal of the working platform, and application of 10 kPa construction load on surface;
4. Dewatering and excavation to underside of the roof slab;
5. Installation of the roof slab (and jet fan niche), and backfill to existing ground surface;
6. Placement of runway fill to design heights (simulated as pressures) with 10 kPa live load above the runway;
7. Staged dewatering and excavation within the diaphragm walls to underside of the base slab;
8. Casting of the base slab and completion of the tunnel structure;
9. Return of the groundwater table to the ground surface and removal of 10 kPa surface loads.

The settlement assessment was undertaken at stage 7, which was considered most critical with maximum excavation under full runway loading.

The assumed levels within the modeled chainage range are summarized in Table 3.

8.4 *Results of analysis*

The deformed mesh of the 3D finite element analysis under the full runway loading and at the final stage of the excavation is shown in Figure 6. The predicted settlement profiles at the top of the roof slab along the diaphragm walls and barrettes prior to casting of the base slab are presented in Figure 7.

The predicted settlement of the tunnel during excavation was about 45 mm on the LHS, 43 mm on the RHS, and 35 mm along the central barrettes. The maximum differential settlement was predicted to be 12 mm between the walls and the barrettes. To allow for uncertainties, the tunnel was designed for a maximum differential settlement of 25 mm. The structural analysis showed that the longitudinal in-plane stiffness of the tunnel would smooth out differential settlements along the tunnel alignment, with the presence of the jet fan niche and variability of the subsurface conditions.

Table 3. Assumed geometry during construction.

Chainage range Feature	5728.8 to 5737.6	5737.6 to 5743.6	5743.6 to 5755.2	5755.2 to 5761.2	5761.2 to 5770.0
	RL (m)				
Natural Ground Level	0.5	0.5	0.5	0.5	0.5
Top of Roof Slab	−0.8	−0.25	+0.4	−0.25	−0.8
Bottom of Roof Slab	−1.8	−1.25	−0.6	−1.25	−1.8
Initial Excavation	−2.8	−2.8	−2.8	−2.8	−2.8
Initial Dewatering	−3.8	−3.8	−3.8	−3.8	−3.8
Intermediate Excavation	−6.0	−6.0	−6.0	−6.0	−6.0
Intermediate Dewatering	−7.0	−7.0	−7.0	−7.0	−7.0
Top of Base Slab	−8.4	−8.4	−8.4	−8.4	−8.4
Bottom of Base Slab	−9.4	−9.4	−9.4	−9.4	−9.4
Final Excavation	−9.7	−9.7	−9.7	−9.7	−9.7
Final Dewatering	−11.7	−11.7	−11.7	−11.7	−11.7
Toe of Diaphragm Wall	−17.0	−17.0	−17.0	−17.0	−17.0

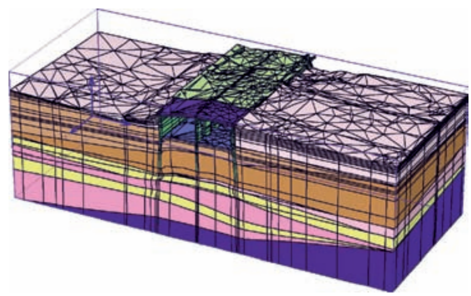

Figure 6. Deformed 3D finite element mesh.

9 FIELD PERFORMANCE

The performance of tunnel during construction was assessed based on the field monitoring results. This was a means to confirm that the structural integrity of the diaphragm walls and barrettes were not adversely affected by differential settlements. Three instrumentation arrays were set up at Ch5655, Ch5718, and Ch5770 corresponding to locations of the runway fill (see Figure 8).

Each array consisted of three settlement plates placed above the LHS and RHS diaphragm walls

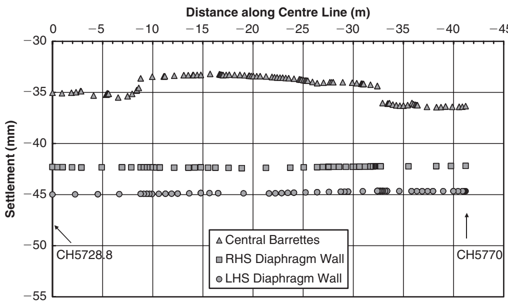

Figure 7. Predicted settlement profiles at top of roof.

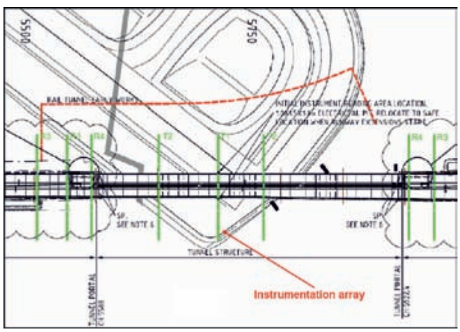

Figure 8. Plan of instrumentation arrays.

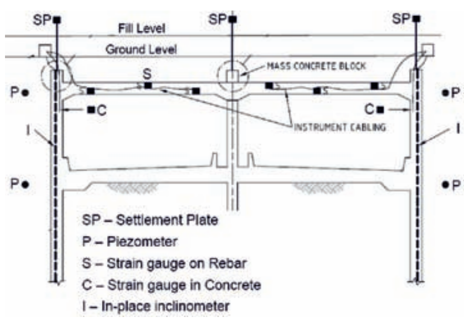

Figure 9. Typical instrumentation section.

and the central barrettes (see Figure 9). These were installed prior to runway fill placement and excavation of the tunnel in order to capture all construction induced movements. In addition to the settlement plates, survey targets were also installed at inner walls to the tunnel to record tunnel movement during excavation. This information had to be calibrated against the settlement plate measurements as the initial tunnel movement record was not available.

Figure 10 shows a summary of construction activities, recorded settlements, and the predicted settlements at diaphragm wall and barrette locations at Ch5718. The settlement prediction adopted here is

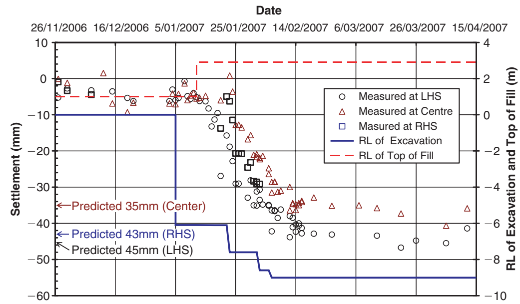

Figure 10. Settlement monitoring results at Ch5718.

the result of analysis between Ch5728.8 and Ch5770. Monitoring commenced at the beginning of November 2006. Excavation of the tunnel commenced in mid December 2006 from the Northern Portal at Ch5588. The excavation process reached Ch5718 in early January. Placement of runway fill above CH5718 followed in mid January, which had resulted in visible settlements of the tunnel. The settlements appeared to have ceased after the excavation reached final depth in mid February. The monitoring data showed that the field performance of the tunnel was consistent with the predictions obtained from the PLAXIS 3D Foundation modelling. Maximum differential settlements between the barrettes and the diaphragm walls were less than 25 mm at all stages of construction.

10 CONCLUSIONS

The Tugun Bypass tunnel had to be constructed under many strict constraints in a challenging geotechnical environment. Extensive site investigations were undertaken to better characterize ground conditions and reduce risks of geotechnical uncertainties. The top-down construction method was adopted to allow extension of the airport runway to occur simultaneously during tunnel construction. The additional loads from the runway fill induced settlements of the tunnel during construction. Settlement analysis of the tunnel using 3D numerical modelling techniques had been undertaken. The differential settlements of the tunnel were successfully predicted. The performance of the tunnel was monitored during construction and the field measurements were consistent with the numerical predictions.

REFERENCES

PLAXIS 2D, Version 8.4, PLAXIS BV Netherlands, 2006.
PLAXIS 3D Foundation, Version 1.6, PLAXIS BV Netherlands, 2006.